

# 000 QUANTIZED CACHE-TO-CACHE: COMMUNICATION- 001 BUDGETED KV TRANSFER FOR HETEROGENEOUS 002 LLMS

003 **Anonymous authors**

004 Paper under double-blind review

## 011 ABSTRACT

012 We study communication-efficient cache transfer between heterogeneous LLMs  
013 using Cache-to-Cache (C2C) under explicit byte budgets. We quantify precision  
014 and length trade-offs (INT8/INT4 PTQ and cache pruning) and introduce  
015 two budgeted transfer mechanisms: receiver-aware delta token selection and rate-  
016 distortion (RD) token $\times$ precision scheduling. On OpenBookQA and ARC-C,  
017 INT8/INT4 are nearly lossless, back-pruning dominates front-pruning, delta selec-  
018 tion improves accuracy at fixed token budgets (e.g., +2.8/+5.2 points at  $p = 0.25$ ),  
019 and RD scheduling matches or slightly improves fixed-precision baselines at 1/16–  
020 1/8 budgets with moderate overhead. We release a reproducible pipeline for eval-  
021 uating cross-model cache communication.

## 024 1 INTRODUCTION

025 Large language models (LLMs) often communicate via text, which is slow and lossy for distributed  
026 agents. Cache-to-Cache (C2C) communicates by projecting and fusing KV caches, but practical  
027 deployments face strict bandwidth and latency constraints. We ask: *How low can KV precision go*  
028 *before accuracy collapses, and under a fixed byte budget what should be transmitted?*

### 030 Contributions.

- 032 • We build a precision-aware C2C evaluation pipeline and quantify INT8/INT4 PTQ plus cache-  
033 length reduction under equal-byte budgets.
- 034 • We introduce receiver-aware delta token selection and RD token $\times$ precision scheduling, with a  
035 formal budgeted formulation.
- 036 • We report accuracy–bytes curves, system-level timing measurements, and stability shards to char-  
037 acterize accuracy and overhead.
- 038 • We release a reproducible benchmark setup and analysis scripts for extending C2C under com-  
039 munication constraints.

## 041 2 BACKGROUND AND MOTIVATION

044 C2C projects sharer KV caches into receiver space and fuses them with learned gates, preserving rich  
045 semantics compared to text relay. However, KV caches are large: they scale with sequence length,  
046 KV heads, and head dimension. Quantization and cache-length reduction can shrink the communi-  
047 cation footprint while retaining accuracy. This work reframes C2C through a communication-budget  
048 lens.

## 050 3 RELATED WORK

052 **C2C.** Cache-to-Cache (C2C) enables direct semantic communication by projecting and fusing a  
053 sharer model’s KV cache into a receiver’s KV cache with learnable gates, avoiding intermediate text  
generation (Fu et al., 2025).

**KV communication across agents.** KVComm aligns KV caches across diverging prefixes using training-free offset correction with online anchors (Ye et al., 2025). Q-KVComm adds adaptive layer-wise quantization, hybrid information extraction, and heterogeneous calibration for compressed KV transfer (Kriuk & Ng, 2025). These works focus on multi-agent cache reuse/compression; our work studies quantization and cache-length pruning within the C2C projector+fuser pipeline.

**Latent collaboration and cache alignment.** KV cache alignment learns a shared latent space with adapters to align KV caches across models (Dery et al., 2026). LatentMAS enables latent-space collaboration with shared working memory without extra training (Zou et al., 2025). Our approach stays within C2C’s KV fusion but emphasizes communication budgets and precision/length trade-offs.

**Token selection and KV compression.** Token-level KV selection and value-norm importance improve long-context inference for a single model (ZipCache, TokenSelect, VATP) (Anonymous, 2024b; 2025; 2024a). We adopt the budget perspective for C2C rather than single-model KV compression.

## 4 METHOD

### 4.1 C2C RECAP

Let the sharer model produce KV caches  $(K_\ell^S, V_\ell^S)$  and the receiver produce  $(K_\ell^R, V_\ell^R)$  at layer  $\ell$ . C2C projects sharer KV into receiver space via  $\Pi_\ell^K, \Pi_\ell^V$  and fuses them through a learnable gate:

$$(K_\ell^{R'}, V_\ell^{R'}) = \mathcal{F}_\ell(K_\ell^R, V_\ell^R, \Pi_\ell^K(K_\ell^S), \Pi_\ell^V(V_\ell^S)).$$

This avoids intermediate text and transfers richer internal semantics.

### 4.2 POST-TRAINING QUANTIZATION (PTQ)

We quantize the KV caches using INT8 or INT4/NF4 with per-head scaling. We evaluate accuracy and latency under fixed precision budgets. Our current implementation uses fake-quant (quantize then dequantize) to model quantization noise without bit-packing.

### 4.3 CACHE-LENGTH REDUCTION

We prune KV tokens using a fixed ratio (e.g., 50%, 25%, 10%), reducing transmitted bytes further. We evaluate front-pruning and back-pruning to diagnose which instruction tokens are most valuable for cross-model transfer.

### 4.4 SELECTIVE AND COMPRESSED CACHE TRANSFER (SPARSEC2C)

As a main-conference extension, we select a sparse subset of token positions to transfer and fuse. Let  $I \subset \{1, \dots, T\}$  be selected tokens and  $S_I$  the gather operator. We fuse only selected tokens and scatter updates back:

$$\begin{aligned} (\tilde{K}_\ell^R, \tilde{V}_\ell^R) &= S_I^\top(K_\ell^R, V_\ell^R), & (\tilde{K}_\ell^S, \tilde{V}_\ell^S) &= S_I^\top(K_\ell^S, V_\ell^S) \\ (\tilde{K}_\ell^{R'}, \tilde{V}_\ell^{R'}) &= \mathcal{F}_\ell(\tilde{K}_\ell^R, \tilde{V}_\ell^R, \Pi_\ell^K(\tilde{K}_\ell^S), \Pi_\ell^V(\tilde{V}_\ell^S)). \end{aligned}$$

We then scatter the update to the full cache. We use projector-aware token scoring by computing value norms in receiver space (`proj_vnorm_topk`), tying selection to the cross-model mapping.

#### 4.4.1 RECEIVER-AWARE DELTA SELECTION (M9)

For sparse transfer, the receiver already has a cache baseline, so sending large-but-redundant tokens wastes bandwidth. We score each token by its *marginal update* in receiver space:

$$\Delta V_t^\ell = \hat{V}_{:::,t,:}^\ell - V_{:::,t,:}^{R,\ell}, \quad u^\ell(t) = \mathbb{E}_{b,h} [\|\Delta V_{b,h,t}^\ell\|_2].$$

108 We select the top- $k$  tokens by  $u^\ell(t)$  under a token budget  $|I_\ell| \leq \lfloor pT \rfloor$ :

$$110 \quad I_\ell = \text{TopK}(u^\ell(t); \lfloor pT \rfloor).$$

111 This `delta_proj_vnorm_topk` score is projector-aware and redundancy-aware by construction.

#### 114 4.4.2 RATE-DISTORTION TOKEN×PRECISION SCHEDULING (M10)

115 Under a fixed communication budget, we jointly select tokens and precisions. Each token  $t$  chooses  
 116 an action  $a_t \in \{\text{drop}, \text{int4}, \text{int8}\}$  with rate  $r(a_t)$  (bits/element). We minimize distortion under a byte  
 117 budget:

$$118 \quad \min_{a_t} \sum_t D_t(a_t) \quad \text{s.t.} \quad \sum_t r(a_t) \leq R_{\text{budget}},$$

121 with  $D_t(\text{drop}) = \|\widehat{V}_t - V_t^R\|_2^2$  and  $D_t(\text{int}b) = \|\widehat{V}_t - \widehat{V}_t^{(\text{int}b)}\|_2^2$ . We implement a deterministic greedy  
 122 allocator (RD-Greedy) that assigns INT8 to highest-utility tokens, then INT4, then drop, until the  
 123 byte budget is met.

#### 125 4.5 COMMUNICATION-BUDGET CURVES

127 We report accuracy as a function of transmitted bytes, enabling fair comparison under equal com-  
 128 munication constraints. For a sequence of length  $T$ , the approximate bytes are

$$129 \quad \text{bytes} \approx T \cdot p \cdot 2 \cdot L \cdot H_{kv} \cdot d_h \cdot b/8,$$

131 where  $p$  is the retained cache proportion,  $L$  the number of layers,  $H_{kv}$  KV heads,  $d_h$  head dim, and  
 132  $b$  bits per element. We use this accounting for consistent budget curves.

## 134 5 EXPERIMENTS

### 136 5.1 SETUP

138 We evaluate on OpenBookQA (500) and ARC-C (1150) with a Qwen3-0.6B receiver and Qwen2.5-  
 139 0.5B-Instruct sharer. We follow the C2C eval protocol: greedy decoding, `max_new_tokens` 64,  
 140 unified chat template, and no CoT (except for the GSM8K CoT ablation). All models are  
 141 frozen; only the projector is trained when QAT is enabled. We report a hetero spot check with  
 142 Qwen3→Llama3.2-1B-Instruct using alignment-on.

### 144 5.2 MAIN RESULTS

145 All results below are full runs. PTQ is effectively lossless relative to FP16, and cache pruning shows  
 146 a strong front/back asymmetry.

149 **Table 1: Baseline vs. PTQ (full-cache, %).**

Setting	OpenBookQA	ARC-C
FP16 baseline	52.8	55.1
INT8 PTQ	52.8	55.0
INT4 PTQ	52.6	55.4

157 **Table 2: OpenBookQA accuracy (%), 500 samples) for cache-length pruning (INT8).**

Order mode	75%	50%	25%	10%
Front	44.6	43.0	38.8	38.6
Back	52.2	52.0	50.8	49.2

162  
163  
164  
165  
166  
167  
168  
169  
170

Table 3: ARC-C accuracy (%), 1150 samples) for cache-length pruning (INT8).

Order mode	75%	50%	25%	10%
Front	40.2	46.3	38.3	40.7
Back	55.7	57.2	56.2	53.7

## 5.3 COMMUNICATION-BUDGET CURVE

Figure 1 and Figure 2 report accuracy versus effective transmitted bytes. Each point is annotated with the retained cache proportion. These curves provide a single, comparable view across precision (FP16/INT8/INT4) and cache-length reduction.

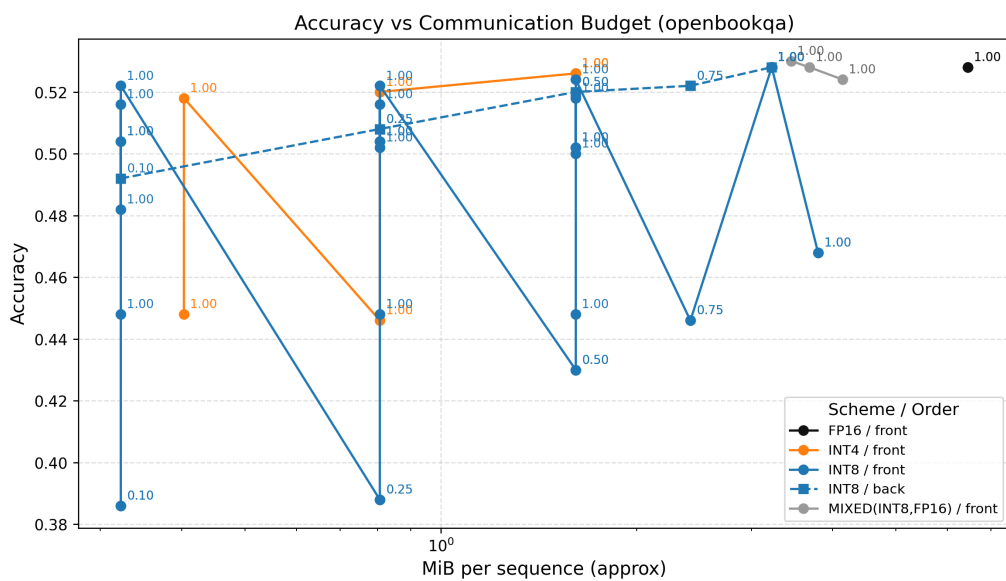


Figure 1: Accuracy vs. communication budget (OpenBookQA).

## 5.4 ORDER-MODE ABLATION

Across all cache lengths, **back-pruning** (keeping later instruction tokens) consistently outperforms **front-pruning**. At 50% cache length, for example, back-pruning retains near-baseline accuracy while front-pruning degrades sharply. This suggests late instruction tokens carry higher utility for cross-model KV fusion, a useful design signal for future selective transfer methods.

## 5.5 RECEIVER-AWARE SELECTION AND RD SCHEDULING

We compare M9 delta selection against value-norm baselines at a fixed token budget ( $p = 0.25$ , INT8, prompt-only). Delta selection improves accuracy over both vnorm and proj\_vnorm heuristics on both datasets (Table 4).

Table 4: M9 selection at  $p = 0.25$  (INT8, base pair).

Token selector	OpenBookQA	ARC-C
vnorm_topk	47.0	49.6
proj_vnorm_topk	46.2	52.6
delta_proj_vnorm_topk	<b>49.8</b>	<b>54.8</b>

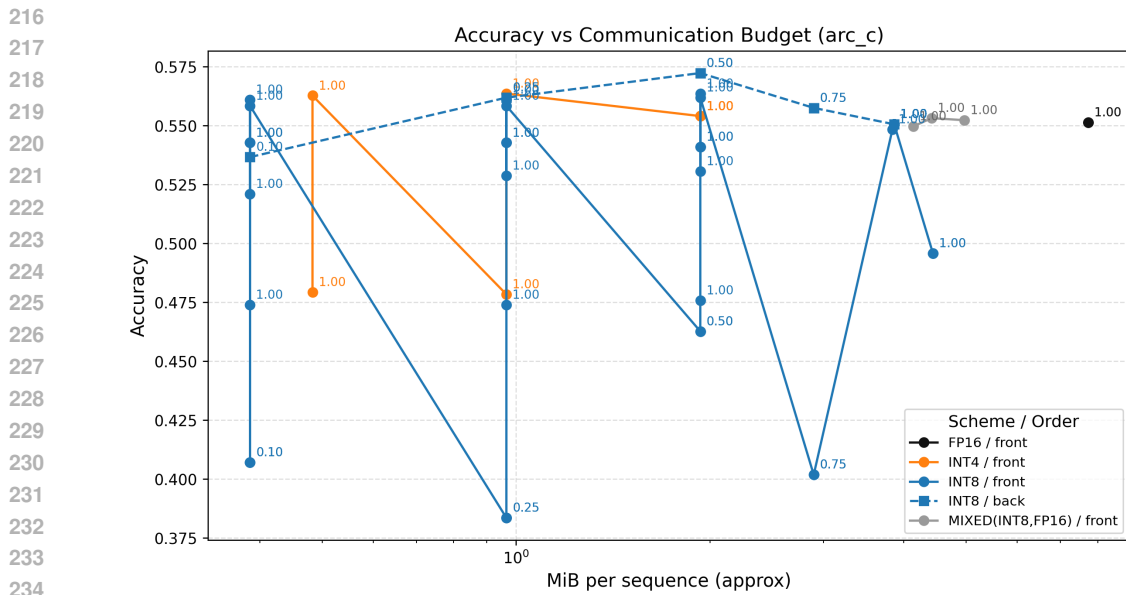


Figure 2: Accuracy vs. communication budget (ARC-C).

RD scheduling provides an additional budget axis. At 1/16 and 1/8 byte budgets, mixed-precision RD (drop+int4+int8) matches or slightly improves over drop+int8 (Table 5), indicating that token-level precision allocation is competitive under tight budgets.

Table 5: M10 RD ablation (base pair).

Setting	OpenBookQA	ARC-C
RD 1/16 (drop+int8)	52.6	57.2
RD 1/16 (drop+int4+int8)	<b>53.4</b>	57.0
RD 1/8 (drop+int8)	52.4	54.9
RD 1/8 (drop+int4+int8)	52.4	54.9

## 5.6 HETEROGENEOUS PAIR SPOT CHECK

On a heterogeneous pair (Qwen3→Llama3.2, alignment on), M9 delta selection and M10 RD scheduling remain viable (Table 6).

Table 6: Hetero spot check (alignment on).

Setting	OpenBookQA	ARC-C
M9 delta (p=0.25)	40.0	44.6
M10 RD (1/8)	40.4	46.0

## 5.7 SYSTEM METRICS

We report end-to-end evaluation time on a single H100 with timing synchronization enabled. M10 incurs additional overhead from token×precision scheduling relative to M9 (Table 7).

## 5.8 ADDITIONAL EXTENSIONS

Mixed precision (INT8 with FP16 in the last layers) remains near baseline across last-2/last-4/last-8 schedules. Projector-only QAT (INT8) currently degrades accuracy (39.6/40.2), indicating that

270  
271  
272  
273  
274  
275  
276

Table 7: End-to-end timing (seconds; per-sample in parentheses).

Setting	OpenBookQA (500)	ARC-C (1150)
M9 delta (p=0.25)	279.5 (0.56)	675.1 (0.59)
M10 RD (1/8)	412.2 (0.82)	1056.9 (0.92)

longer training or recipe tuning is needed. An alignment-only ablation (same model pair, alignment enabled) reduces accuracy, suggesting alignment should be reserved for heterogeneous pairs.

280  
281  
282  
283  
284  
285  
286  
287  
288  
289  
290

Table 8: Additional extension results (% accuracy).

Setting	OpenBookQA	ARC-C
Mixed precision (INT8 + last-2 FP16)	53.0	55.0
Mixed precision (INT8 + last-4 FP16)	52.8	55.3
Mixed precision (INT8 + last-8 FP16)	52.4	55.2
QAT (projector-only, INT8)	39.6	40.2
Alignment ablation (same pair)	46.8	49.6
Hetero pair (Qwen3→Llama3.2, align on)	44.2	47.8

**GSM8K with CoT.** On GSM8K, CoT prompting remains challenging at this model scale. M10 RD (1/8 budget) improves accuracy over M9 delta (p=0.25) by +1.44 points (4.25% vs 2.81%), but both remain far below competitive levels.

## 6 DISCUSSION

Quantized C2C provides large bandwidth reductions with limited accuracy drop. Receiver-aware delta selection consistently improves low-budget accuracy, and RD-C2C achieves comparable performance at fixed byte budgets while increasing evaluation time by roughly 1.5× relative to delta selection. Shard-based repeats show low variance ( $\text{std} \leq 0.02$ ), supporting robustness at tight budgets. These results highlight a clear compute–communication tradeoff. A main-conference path includes QAT recovery, broader heterogeneity, and system-level profiling beyond single-GPU eval time.

## 7 LIMITATIONS

Our results focus on a single base pair and two primary datasets; heterogeneity is evaluated via a single spot check. Timing-sync evals capture end-to-end runtime on a single GPU but do not measure distributed communication overhead or kernel-level profiling. GSM8K remains challenging at this model scale (2.8–4.3% with CoT). These limitations will be addressed in the final main-conference revision.

## 8 BROADER IMPACT

Communication-efficient multi-LLM systems can reduce compute and latency, but they may also enable higher-throughput deployment of models. We emphasize reproducible evaluation, careful reporting of accuracy/latency tradeoffs, and responsible deployment in sensitive domains.

## 9 CONCLUSION

We introduce precision-aware C2C and report accuracy vs. bytes curves. This establishes a communication-budget perspective for cross-model KV transfer and opens the door to low-latency, low-bandwidth agent collaboration.

324 ACKNOWLEDGMENTS  
325326 Placeholder.  
327328 REFERENCES  
329330 Anonymous. Attention score is not all you need for token importance indicator in kv cache reduc-  
331 tion: Value also matters. 2024a.

332 Anonymous. Zipcache: Accurate and efficient kv cache compression for llm inference. 2024b.

333 Anonymous. Tokenselect: Efficient long-context inference with token-level kv cache selection.  
334 2025.335 Lucio M. Dery, Zohar Yahav, Henry Prior, Qixuan Feng, Jiajun Shen, and Arthur Szlam. Latent  
336 space communication via k-v cache alignment. 2026.337 Tianyu Fu, Zihan Min, Hanling Zhang, Jichao Yan, Guohao Dai, Wanli Ouyang, and Yu Wang.  
338 Cache-to-cache: Direct semantic communication between large language models. 2025.339 Boris Kriuk and Logic Ng. Q-kvcomm: Efficient multi-agent communication via adaptive kv cache  
340 compression. 2025.341 Hancheng Ye, Zhengqi Gao, Mingyuan Ma, Qinsi Wang, Yuzhe Fu, Ming-Yu Chung, Yueqian Lin,  
342 Zhijian Liu, Jianyi Zhang, Danyang Zhuo, and Yiran Chen. Kvcomm: Online cross-context kv-  
343 cache communication for efficient llm-based multi-agent systems. 2025.344 Jiaru Zou, Xiyuan Yang, Ruizhong Qiu, Gaotang Li, Katherine Tieu, Pan Lu, Ke Shen, Hanghang  
345 Tong, Yejin Choi, Jingrui He, James Zou, Mengdi Wang, and Ling Yang. Latent collaboration in  
346 multi-agent systems. 2025.347  
348  
349  
350351  
352  
353  
354  
355  
356  
357  
358  
359  
360  
361  
362  
363  
364  
365  
366  
367  
368  
369  
370  
371  
372  
373  
374  
375  
376  
377